View Article Online
View Journal

Green Chemistry

Cutting-edge research for a greener sustainable future

Accepted Manuscript

This article can be cited before page numbers have been issued, to do this please use: O. Oyola-Rivera, J. He, G. Huber, J. Dumesic and N. Cardona-Martínez, *Green Chem.*, 2019, DOI: 10.1039/C9GC01526D.

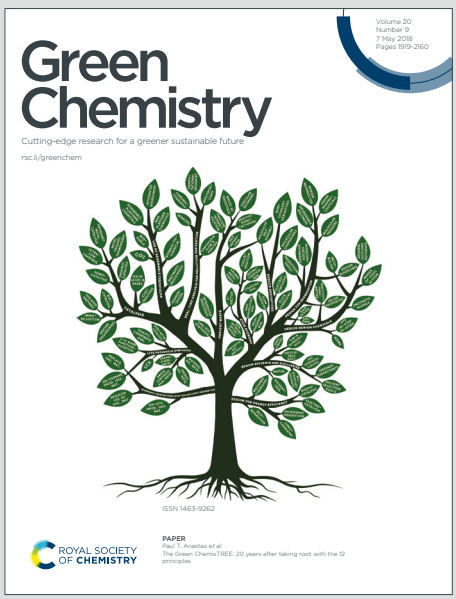

View Article Online
DOI: 10.1039/C9GC01526D

Catalytic dehydration of levoglucosan to levoglucosenone using Brønsted solid acid catalysts in tetrahydrofuran

Oscar Oyola-Rivera[a], Jiayue He[b], George W. Huber[b], James A. Dumesic[b], and Nelson Cardona-Martínez[a]*

E-mail addresses: oscar.oyola@upr.edu (O. Oyola-Rivera), jiayue.he@wisc.edu (Jiayue He), jdumesic@wisc.edu (James A. Dumesic), gwhuber@wisc.edu (George W. Huber), and nelson.cardona@upr.edu (N. Cardona-Martínez)

Abstract

We studied the production of levoglucosenone (LGO) *via* levoglucosan (LGA) dehydration using Brønsted solid acid catalysts in tetrahydrofuran (THF). The use of propylsulfonic acid functionalized silica catalysts increased the production of LGO by a factor of two compared to the use of homogeneous acid catalysts. We obtained LGO selectivities of up to 59% at 100% LGA conversion using solid Brønsted acid catalysts. Water produced during the reaction promotes the solvation of the acid proton reducing the activity and the LGO production. Using solid acid catalysts functionalized with propylsulfonic acid reduces this effect. The hydrophilicity of the catalyst surface seems to have an effect in reducing the interaction of water with the acid site, improving the catalyst stability.

[a]*Department of Chemical Engineering, University of Puerto Rico, Mayagüez, PR, 00681-9000, Puerto Rico*

[b]*Department of Chemical and Biological Engineering, University of Wisconsin, Madison, WI, 53706, United States*

*Corresponding author.

View Article Online
DOI: 10.1039/C9GC01526D

1. Introduction

Lignocellulosic biomass is one of the most abundant carbon sources in the world and has the potential of becoming an important source for the renewable production of commodity chemicals and transportation fuels.[1–5] Biomass may be obtained from forestry resources, agricultural residues, energy crops, and industry wastes.[6,7] Levoglucosenone (LGO) is a platform molecule that can be produced from cellulose by different catalytic routes.[5,8–11] LGO is an anhydrous sugar that has been used as a feedstock for the synthesis of pharmaceuticals, 1,6-hexanediol (a polymer precursor), and Cyrene™ (a solvent).[5,8,10,12–14] LGO is commonly produced from the catalytic pyrolysis of cellulose and the yield obtained for LGO is typically low (less than 20%).[10,11,15] Recently, Huber and co-workers, obtained yields of 38%, for LGO from cellulose in tetrahydrofuran (THF) in the absence of water using sulfuric acid as catalyst.[8] However, the LGO yield decreased from 38% to less than 15% as the cellulose loading increased from 1 to 10 wt%.[8]

LGO is produced from the dehydration of levoglucosan (LGA) during the conversion of cellulose in the presence of an acid catalyst and in the absence of water.[5,8,16,17] LGA is an anhydrous sugar that is mainly produced from cellulose by fast pyrolysis, at yields of up to 45%.[18] The production of LGO has been mainly studied via acid-catalyzed pyrolysis of LGA and cellulose using acid catalysts.[11,15,19–21] Two routes have been proposed for the acid-catalyzed conversion of LGA to LGO. LGA may be directly dehydrated to LGO or iso-LGO, or it can be dehydrated to 1,4:3,6-dianhydro-a-D-glucopyranose (DGP) followed by the dehydration of DGP to LGO.[5,16,17]

Cao *et al.,* studied the production of LGO from LGA using 20 mM sulfuric acid in tetrahydrofuran (THF) and water.[5] They obtained LGO yields of up to 50% starting with

View Article Online
DOI: 10.1039/C9GC01526D

0.4 wt% LGA in pure THF.[5] By adding 2.7 wt% water in THF, the LGO yield decreases from 50% to around 22% due to the hydrolysis of LGA to glucose and the production of 5-hydroxymethylfurfural (HMF) from glucose.[5] These observations show that the presence of water adversely affects the production of LGO from LGA. However, water production during the reaction is unavoidable since LGO is produced from LGA through a dehydration reaction. Therefore, we used an acid catalyst, with similar properties found for sulfuric acid such as propylsulfonic acid, supported on silica with hydrophilic silanol groups that may help to reduce the effects of water during the reaction.[22] Using a solid catalyst also facilitates the separation of products and reduces exposure during the process to corrosive liquid species such as sulfuric acid.

In this study, we explored the use of solid Brønsted acid functionalized silica catalysts for the dehydration of LGA to LGO in THF. Using acid functionalized silica catalysts, we obtained LGO selectivities of up to 68% at 58% LGA conversion. We observed that the silica surface silanol groups interact with the water produced during the reaction, reducing the interaction of water with the acid sites and catalyst deactivation. We demonstrated that the surface properties of acid functionalized silica catalysts such as hydrophilicity and hydrophobicity affect LGO production.

2. Experimental

2.1. Catalysts preparation

Propyl sulfonic-functionalized mesoporous silica (PS-SBA-15) was synthesized using the one-step synthesis procedure reported by Stucky and co-workers.[23] In this synthesis, 15 g of Pluronic P123 (Sigma-Aldrich) were dissolved in 480 mL of 2.0 M HCl (Acros Organics, 37% solution in water) and 24 mL of DI water. The mixture was heated

View Article Online
DOI: 10.1039/C9GC01526D

to 313 K and stirred for 3 h. Then 25 mL of tetraethyl orthosilicate (TEOS) (Acros Organics, 98% purity) were added dropwise to the P123 solution and pre-hydrolyzed for 45 min at 313 K under stirring. Following the pre-hydrolysis of TEOS, 4.8 mL of (3-mercaptopropyl)trimethoxysilane (MPTMS) (Alfa Aesar, 95% purity) and 7.3 mL of 30 wt% H_2O_2 (Fisher Chemical, 30% certified ACS) solution were added dropwise to the suspension. The mixture was aged at 313 K for 20 h under stirring. The temperature of the mixture was increased to 373 K and aged for an additional 20 h under stirring. The precipitated solid was filtered and washed with DI water and dried overnight at room temperature under vacuum. The copolymer template (P123) was removed by refluxing with 4 L of ethanol for 24 h. Following the removal of the copolymer template, the solid was filtered and washed with 2 L of fresh ethanol. Finally, the solid was dried for 24 h at 353 K under vacuum.

The non-functionalized SBA-15 was synthesized using the same procedure described above for PS-SBA-15 without adding the MPTMS and H_2O_2. The aged precipitated solid was washed with DI water and dried at 373 K overnight under vacuum. The dried solid was calcined for 6 h at 823 K in air with a heating ramp of 3 K/min.

We used commercial acid-functionalized catalysts SiliaBond® from SiliCycle as received. These catalysts are amorphous silica gels functionalized with propylsulfonic acid (SiliaBond®-PSA) and arenesulfonic acid (SiliaBond®-Tosic-a).[24] We used commercial available non-endcapped (SiliaBond®-PSA, R51430B) and endcapped (SiliaBond®-PSA, R51230B and SiliaBond®-Tosic-a, R60530B) samples. The non-endcapped catalysts have acid functionality and residual silanol groups (surface hydroxyl groups that did not react during the functionalization).[24] The endcapped catalysts have acid functionality and

View Article Online
DOI: 10.1039/C9GC01526D

trimethylsilyl groups instead of silanol groups.[24] The synthesis procedure for these catalysts consists of the functionalization of a fraction of the silanol groups with the acid precursor followed by the functionalization of the residual silanol groups with trimethylsilychloride to form trimethylsilyl groups.[24] The endcapping reduces the acidity and polarity on the silica surface and should make it more stable.[24]

2.2. Catalyst characterization

Nitrogen physisorption isotherms at 77 K were obtained using an accelerated surface area and porosimetry system Micromeritics ASAP 2020 unit. The BET surface areas were determined using adsorption data at relative pressures between 0.10 and 0.25. The total pore volume was estimated from the amount of N_2 adsorbed at a relative pressure of 0.99. The micro and mesopore volumes were determined using the α_s-plot method.[25–27] The mesopore diameter was estimated from a pore size distribution (PSD) analysis including the correction of the Kruk-Jaroniec-Sayari (KJS) for the statistical film thickness in the Barret-Joyner-Halenda (BJH) method.[28] The pore wall thickness was estimated by calculating the difference between the lattice cell parameter and the pore diameter.

The powder X-ray diffraction studies were performed using a Bruker D8 Discover X-Ray diffractometer equipped with cross beam optics and a Cu K_α target, operating at 50 kV and 1000 μA to study the ordered mesoporous structure of the samples. Powder diffraction patterns using small angle mode were determined from 0 to 5° 2θ angles.

The acid loading of 0.10 g of propyl sulfonic acid functionalized SBA-15 was determined by ion exchange with 20 mL of an aqueous solution of 2 M NaCl (Fisher Chemical, certified ACS) for 2 h and titration with an aqueous solution of 0.01 M NaOH (Acros Organics, 98.5% purity).

View Article Online
DOI: 10.1039/C9GC01526D

The samples were chemically analyzed by inductively coupled plasma optical emission spectroscopy (ICP-OES) using a Varian Vista-MPX ICP-OES to obtain the sulfur loadings on the catalysts. The samples were pretreated by acid digestion at 393 K overnight. In a typical experiment, around 15 mg of catalyst were digested with a mixture of 1 mL of 37% hydrochloric acid solution (ACS reagent, Sigma-Aldrich), 1 mL of 70% nitric acid solution (ACS reagent, Sigma-Aldrich) and 1 mL 48% hydrofluoric acid solution (99.99% trace metal basis, Sigma-Aldrich).

2.3. Catalytic performance

The catalytic conversion of levoglucosan was studied using a 100 mL Parr Instrument model 4565 high-pressure batch reactor. The reactor was heated using a 500 W rigid heating mantle. The temperature and stirring were controlled using a Parr Instrument model 4848 closed loop temperature controller. The temperature was measured using an Omega JQSS-M30G-300 Type J thermocouple of 1/8 in diameter. The reactor was stirred using a four-blade impeller with a 1/8 HP motor. The levoglucosan (CarboSynth, 98% purity), catalysts and reactor were dried at 358 K overnight before the reactions. The LGA solutions were prepared using 139, 349 and 867 mg of LGA to obtain concentrations of 14, 36 and 89 mM LGA in THF (Alfa Aesar, ACS 99% stabilized with BHT), respectively. The solid acid catalyst loading was adjusted to 0.08 mmol H^+ in 60 mL of THF. In a typical experiment, the desired amount of LGA and solid catalyst, previously dried, were added to the reactor followed by the addition of 60 mL of THF. Then, the reactor was closed and purged with He (99.999%, Airgas) 5 times. The reactor was pressurized to 34 bar and heated to the desired temperature and pressurized with He to 69 bar. The stirring rate was maintained at 700 rpm. The zero time was set to the point when we started to heat the

View Article Online
DOI: 10.1039/C9GC01526D

reactor. Samples of around 0.5 mL were taken periodically via dip tube and quenched in a dry ice-bath and filtered with 0.22 μm syringe filter (Restek, PTFE (polytetrafluoroethylene)). The reactor was quenched in an ice-water bath after reaction.

2.4. Thermal stability tests

The thermal stability of propyl sulfonic acid functionalized SBA-15 in THF was investigated by exposing the catalyst sample to THF at 483 K and 69 bar of He for various treatment times (40, 70 and 100 min). Then each sample was filtered and washed with THF to remove the physisorbed species on the catalyst surface. Finally, the solid was dried at 353 K under vacuum overnight. The solid was then characterized using XRD, BET, ICP and acid-base titration to determine any change in the structural and acid properties of the material.

2.5. Analytical methods

The soluble products were analyzed using a high-performance liquid chromatograph (Shimadzu LC-20AT) equipped with an UV (UV-vis SPD-20AV) and refractive index (RID-10A) detectors. The reaction products were separated with a packed carbohydrates analysis column (Bio-Rad Aminex HPX-87H) using 5 mM H_2SO_4 aqueous solution as the mobile phase at a flow rate of 0.6 mL/min and a column temperature of 303 K. The LGA concentration was measured using a refractive index detector. HMF and furfural were identified and quantified using their UV spectra at 280 nm. LGO was identified and quantified using its UV spectrum at 370 nm. No other products were detected using refractive index and UV detectors. The sample injection volume was 1 μL.

The conversion of LGA was calculated as follows:

View Article Online
DOI: 10.1039/C9GC01526D

$$X_{LGA}(\%) = \frac{C_{LGA,\ 0} - C_{LGA}}{C_{LGA,\ 0}} x\ 100(\%)$$

where $C_{LGA,\ 0}$ is the initial carbon concentration of LGA and C_{LGA} is the carbon concentration of LGA at each sampling time. The yield and selectivity corresponding to each detectable product *i* were calculated as follows:

$$Y_i(\%) = \frac{C_i}{C_{LGA,\ 0}} x\ 100(\%)$$

$$S_i(\%) = \frac{C_i}{C_{LGA,\ 0} - C_{LGA}} x\ 100(\%)$$

where C_i is the carbon concentration of each detectable product i. The turnover frequency (TOF) towards LGO based on the Brønsted acid concentrations (C_{H+}) were estimated as follows:

$$TOF_i = \frac{1}{C_{H^+}} \frac{dC_i}{dt}$$

using the change in LGO concentration with time after the reaction reached 483 K at 40 min of reaction. The TOF of LGA consumption based on the Brønsted acid concentrations were estimated as follows:

$$TOF_{LGA} = \frac{1}{C_{H^+}} \frac{dC_{LGA}}{dt}$$

using the change in LGA concentration with time after reaching 483 K at 40 min of reaction.

3. Results and discussion

3.1. Catalyst Characterization

Table 1 summarizes the physicochemical properties for the functionalized SBA-15 as well as for the commercial silica catalysts. The presence of Brønsted acid sites on PS-

View Article Online
DOI: 10.1039/C9GC01526D

SBA-15 confirms the incorporation and the oxidation of MPTMS on the catalysts surface. The N_2 adsorption isotherms obtained for SBA-15 and PS-SBA-15 catalysts are both type IV with an H_1 hysteresis that correspond to average pore diameters inside the mesoporous region. The functionalized PS-SBA-15 exhibits a lower average pore diameter compared to that obtained for non-functionalized SBA-15. This difference may be attributed to the incorporation of the organofunctional groups on the pore surface.[29] The surface area of functionalized PS-SBA-15 is lower than that obtained for non-functionalized SBA-15. The wall thickness for the PS-SBA-15 is higher than for SBA-15. The difference in the surface area and pore wall thickness is consistent with the presence of the propylsulfonic groups on the catalyst pore surface. The external surface area for PS-SBA-15 is almost four times higher than that obtained for SBA-15. It is possible that the particles of PS-SBA-15 are smaller than the SBA-15 particles. The micropore volume for PS-SBA-15 is lower than that obtained for SBA-15. The micropores channels may be blocked by the MPTMS groups or by residual copolymer template P123. The copolymer template was removed by calcination for the non-functionalized SBA-15. On the other hand, for PS-SBA-15, the copolymer template was removed using a reflux of ethanol. The calcination treatment is typically more effective in removing the copolymer template completely from micropores, obtaining a less dense material and a free path through the micropores channels.

Table 1. Physicochemical properties of solid acid catalysts[a]

Catalyst	C_{H+}[b] (mmol/g)	S_{BET} (m^2/g)	S_{Ext}[c] (m^2/g)	D_p (nm)	W_p[c] (nm)	$V_{P/Po=0.99}$ (cm^3/g)	V_p[d] (cm^3/g)	V_m[d] (cm^3/g)
SBA-15	-	855	6	7.9	3.7	0.05	0.03	0.01
PS-SBA-15	0.96	734	26	5.8	5.6	0.63	0.59	0.00
SiliaBond®-PSA non-endcapped	0.71	279	9	7.8	9.3	0.43	0.42	0.00
SiliaBond®-PSA endcapped	0.62	420	15	7.2	9.4	0.58	0.57	0.00
SiliaBond®-Tosic-a endcapped	0.61	238	4	7.2	8.6	0.28	0.28	0.00

[a]C_{H+} is the content of Brønsted acid sites on the catalyst surface per gram of catalyst, S_{BET} is the BET surface area, S_{Ext} is the external surface area, D_p is the mesopore diameter, W_P is the pore wall thickness, $V_{P/Po=0.99}$ is the total pore volume estimated from the amount of N_2 adsorbed at a relative pressure of 0.99, V_p is the mesopore volume, and V_m is the micropore volume.
[b]Determined by titration.
[c]The pore wall thickness was calculated using the distance between pores (*a*) calculated based on the d_{100} interplanar spacing and assuming hexagonal geometry.
[d]Calculated using the α_s-plot method using the standard parameters corresponding to mesoporous silica.

View Article Online
DOI: 10.1039/C9GC01526D

The XRD patterns for non-functionalized and acid-functionalized silica are shown in Figure 1. The XRD pattern corresponding to non-functionalized SBA-15 exhibits the (100), (110) and (200) peaks that correspond to an ordered hexagonal array, p6mm.[29,30] The acid functionalized PS-SBA-15 only shows the (100) peak at $2\theta = 0.9$ confirming the presence of an ordered hexagonal array. The (100) peak for PS-SBA-15 is not as sharp as that obtained for SBA-15. This may be attributed to the incorporation of organofunctional groups on PS-SBA-15.[30] The absence of the long-ordered reflection peaks (110) and (200) for PS-SBA-15 may be attributed to a less ordered mesostructure resulting from the co-condensation synthesis method.[31,32]

The physicochemical properties of SiliaBond catalyst are summarized in Table 1. It has been reported that SiliaBond catalysts have a non-ordered porous structure.[24] We observed that the average pore diameter for the SiliaBond catalyst is between 7.2 and 7.8 nm. The N_2 adsorption isotherms for these catalysts are of type IV, which is characteristic of a mesoporous structure. The micropore volume for these catalysts was zero, confirming the absence of pores with diameter ≤ 2 nm. Based on these results we conclude that the porosity of these materials is mainly within the mesoporous range. The XRD patterns for SiliaBond catalysts exhibit only one broad diffraction peak around $2\theta = 0.8$, as shown in Figure 1. This peak may be attributed to the low order of the pores, which is consistent with the manufacturer's description.

[Figure 1 near here]

View Article Online
DOI: 10.1039/C9GC01526D

3.2. Catalytic Performance

3.2.1. Homogeneous catalytic dehydration of LGA

Huber and co-workers studied the use of sulfuric acid for the conversion of cellulose to LGO in polar aprotic solvents.[5,8] They compared the catalytic performance of sulfuric, phosphoric, formic, and hydrochloric acids for the conversion of cellulose to LGO in THF.[8] The highest yield for LGO was obtained when H_2SO_4 was used as the catalyst. They also studied the conversion of cellulose to LGO using H_2SO_4 in different polar aprotic solvents. The highest yield obtained for LGO was in THF; this was attributed to a lower rate of LGO degradation in THF compared to the other polar aprotic solvents.[8] We studied the conversion of LGA to LGO using sulfuric acid to have a reference of the LGO yields that can be obtained with the catalyst that showed a better performance for the production of LGO from cellulose in THF reported in the literature. For comparison we also studied the conversion of LGA to LGO using 1-propanesulfonic. 1-Propanesulfonic acid is a liquid acid analogous to the functional groups present on PS-SBA-15. This comparison will help to understand the effect of having those functional groups on the surface of a solid acid catalyst.

Figure 2 shows the LGA conversion and products selectivity as a function of reaction time obtained using homogeneous acid catalysts. The amount of catalyst was fixed to have the same concentration of Brønsted acid in each experiment. When using sulfuric acid as the catalyst, two regions with different reaction rates were observed. Initially, the average TOF from 40 to 100 min was 0.7 ks^{-1}. After 100 min of reaction the average TOF decreases to 0.1 ks^{-1} and the maximum conversion obtained was 51.5%. For 1-propanesulfonic acid, three regions with different reaction rates were observed. Initially, a

View Article Online
DOI: 10.1039/C9GC01526D

slow LGA conversion rate was observed with an average TOF of 0.1 ks^{-1} from 40 to 50 min, followed by an increment in the TOF to 1.4 ks^{-1} from 50 to 90 min. At 90 min the TOF decreases to 0.4 ks-1, this behavior is similar to that observed for sulfuric acid. The maximum LGA conversion obtained using 1-propanesulfonic acid was 54.5% at 160 min. These observations suggest that the acid proton may have been stabilized during the reaction reducing its reactivity. This effect may be attributed to the formation of water during the reaction. Mellmer et al., proposed that the lower reactivity of an acid proton in water can be attributed to high proton solvation by water molecules.[22] They also proposed that the reactivity of an acid proton may be reduced due to a higher stabilization of the proton in water than in a polar aprotic solvent.[22] Hence, we speculate that the reactivity of the sulfuric acid protons decreases as the water content increases during the reaction reducing the rate of LGA conversion.

[Figure 2 near here]

The LGO selectivity using 1-propanesulfonic acid (33%) and sulfuric acid (33%) were almost the same at a similar LGA conversion (around 49%). The HMF and furfural selectivities were 1% and 0% for 1-propanesulfonic acid and 7% and 1% for sulfuric acid at 49% conversion. The selectivity for non-detectable products at the same conversion was 65% and 59% for 1-propanesulfonic and sulfuric acids, respectively. For sulfuric acid the production of non-detectable products increases as the LGO, HMF and furfural selectivities decrease with time, suggesting that the main reaction routes for their production comes primarily from the degradation of the detectable products. The average rate of LGA consumption at 40 min, when the 483 K temperature set point was reached, is 7 times higher for sulfuric acid than for 1-propanesulfonic acid. These results indicate that sulfuric

View Article Online
DOI: 10.1039/C9GC01526D

acid is more active for the conversion of LGA compared to 1-propanesulfonic acid. The higher production of HMF and furfural using sulfuric acid may also be attributed to its higher activity (between 40 and 60 min) compared to 1-propanesulfonic acid and can promote the conversion of LGO to HMF, furfural and non-detectable products. Sulfuric acid is a stronger Brønsted acid catalyst (pK_a = -3.0) compared to 1-propanesulfonic acid (pK_a = -1.5).[22] The difference in the catalyst activity at the beginning of the reaction can thus be attributed to a higher proton solvation in THF when sulfuric acid is used as catalyst compared to 1-propanesulfonic acid. These observations are in agreement with the conversion of sugars in polar aprotic solvents previously studied by Mellmer et al.[22] It has to be pointed out that this observation only applies to the initial reaction rates. For our experimental conditions we calculate the initial reaction rates at 40 min of reaction because that is the time when we reach the temperature set point. Before 40 min of reaction, the temperature is increasing and a reliable estimation of the TOF cannot be obtained. Also, at 40 min of reaction the production of water is still low and the stabilization effect of water on the acid proton is lower. After 50 min of reaction the TOF for 1-propanesulfonic acid is higher compared to that obtained for sulfuric acid. This difference can be related to the stabilization of sulfuric acid proton due to the production of water, as explained above. From this point, we believe that the low production of HMF and furfural, and the higher production of degradation products using 1-propanesulfonic acid compared to sulfuric acid is related to its higher activity. The degradation of HMF and furfural to non-detectable products using 1-propanesulfonic acid may be higher, showing low selectivities towards HMF and furfural.

View Article Online
DOI: 10.1039/C9GC01526D

3.2.2. LGA dehydration using acid-functionalized silica

The dehydration of LGA was studied using functionalized ordered porous SBA-15 and commercial functionalized non-ordered porous silica (SiliaBond). The conversion of LGA using non-functionalized SBA-15 was around 2% after 190 min of reaction. LGO was not produced using non-functionalized SBA-15. Trace amounts of HMF and furfural were observed during the reaction, with selectivities of up to 14% and 3% for HMF and furfural, respectively. In the absence of a catalyst, no LGA conversion was detected. It has been suggested that the silanol groups on SBA-15 surface can act as acid sites with similar acid properties to those of acetic acid.[29] The low production of HMF and furfural may be attributed to the presence of weak acidic hydroxyl groups on SBA-15.

Figure 3 shows the conversion and product selectivities obtained for LGA dehydration for different LGA concentrations using PS-SBA-15. The reaction time to obtain full conversion increased from 70 min for 14 mM LGA to 80 min for 36 mM LGA. The maximum conversion achieved was 83% for 89 mM LGA feed at a reaction time of 160 min. The LGO selectivities, at similar LGA conversion, were obtained using initial LGA concentrations of 14, 36 and 89 mM were 68% (X_{LGA}=58%), 39% (X_{LGA}=65%), and 37% (X_{LGA}=66%), respectively. Increasing the concentration of LGA results in a decrease in the LGO selectivity. After reaching the maximum LGA conversion, the LGO and HMF selectivities start to decrease as shown in Figure 3a and 3b. However, the selectivity towards furfural increases after the LGA was completely consumed, suggesting that the furfural produced comes from LGO or HMF and it is promoted by the presence of the acid catalyst. The average TOF for the consumption of LGA, when the reaction set point was reached, rises as the initial LGA concentration increases, as shown in Figure 7. These

View Article Online
DOI: 10.1039/C9GC01526D

results suggest that the apparent reaction order for the dehydration of LGA is near 1. The selectivity towards LGO decreases as the TOF for LGA consumption increases, while the selectivity towards non-detectable products increases. As the catalyst dehydration activity increases the conversion of LGO to degradation products increases.

[Figure 3 near here]

LGA was not completely consumed when the feed was 89 mM LGA, with a maximum LGO selectivity (37%) obtained before the LGA conversion reached a plateau. After that time, the LGO selectivity decreased from 37% to approximately 33% and remained constant until a new plateau at around 24% was observed. The decrease in LGO selectivity with an initial LGA concentration of 89 mM (approximately 2% decrease) is lower compared to the decrease in LGO selectivity using 14 and 36 mM LGA initial concentrations (approximately 33% to 36%). We attribute this behavior to the deactivation of the catalyst due to the production of water during the reaction. The rise in water concentration can promote an interaction between water and the acid proton, thus stabilizing it and reducing its catalytic activity, similar to the behavior observed for sulfuric acid. Based on the LGA consumed during the reaction, we estimated the amount of water produced during the reaction, as shown in Figure 4a. Contrary to the selectivity, the amount of LGO produced is higher as the initial concentration of LGA increases. Hence, the production of water increases as the initial LGA concentration increases. These results suggest that the catalyst is deactivating due to a higher production of water when an initial concentration of 89 mM LGA is used. The results also suggest that the consumption of LGO starting with 14 and 36 mM LGA may be attributed to the presence of the remaining active proton sites on the catalyst once the LGA is completely consumed. From these

View Article Online
DOI: 10.1039/C9GC01526D

observations, we also conclude that the LGO degradation in the presence of water and THF at 483 K is low in the absence of active acid species.

[Figure 4 near here]

The conversion and selectivities obtained for the dehydration of LGA using commercial non-endcapped SiliaBond®-PSA are shown in Figure 5. The maximum LGO selectivity obtained with non-endcapped SiliaBond®-PSA was 52%. The TOF for LGA consumption and the TOF for LGO were 2.7 ks^{-1} and 1.2 ks^{-1}, respectively. The TOF for LGA consumption obtained using non-endcapped SiliaBond®-PSA (2.7 ks^{-1}) is similar to that obtained for PS-SBA-15 (2.3 ks^{-1}). This result suggests that the structural properties of the silica support do not have a significant effect on the acid site activity. The selectivity towards LGO obtained using non-endcapped SiliaBond®-PSA was 49% at 100% conversion. This selectivity is lower compared to that obtained using PS-SBA-15 (59%) at 100% conversion. While the selectivity towards non-detectable products at 100% conversion is higher (44%) compared to that obtained for PS-SBA-15 (31%). Also, after reaching full LGA conversion, the LGO selectivity decreases from 49% to 21%, while when using PS-SBA-15 the LGO selectivity decreases from 59% to 34%. The degradation of LGO using non-endcapped SiliaBond®-PSA is higher compared to that for PS-SBA-15. This behavior may be related to the lower concentration of hydroxyl groups on non-endcapped SiliaBond®-PSA (3 mmol OH/g) surface compared to on PS-SBA-15 (8 mmol OH/g). The hydroxyl groups are hydrophilic species that may attract the water produced during the reaction to the catalyst surface. Hence, increasing the hydroxyl groups concentration can lead to the interaction of more water molecules with the catalyst surface reducing the interaction with LGO and reducing its degradation. Additionally, we note that

View Article Online
DOI: 10.1039/C9GC01526D

the production of furfural increases after LGA was completely consumed while the LGO concentration decreases using non-encapped SiliaBond®-PSA, as observed using PS-SBA-15, confirming that a considerable fraction of the furfural produced comes from LGO.

[Figure 5 near here]

The results obtained for the dehydration of 14 mM LGA using endcapped SiliaBond®-PSA are shown in Figure 6a. The maximum selectivity obtained for LGO was 59%. This selectivity is higher than that obtained for non-endcapped SiliaBond®-PSA (49%). The average TOF at 40 min for the consumption of LGA (2.7 ks^{-1}) is the same compared to that obtained using the non-endcapped catalysts and similar to that for PS-SBA-15. These results suggest that the trimethylsilyl functionalization does not have a significant effect on the acid site activity. However, the incorporation of trimethylsilyl groups on the catalysts surface reduces the presence of hydroxyl groups on the catalyst surface. The silyl ether groups may reduce the interaction of water with the catalyst surface due to an increase in the hydrophobicity on the catalyst surface.[34] These properties may help to reduce the interaction of water with the acid sites and LGO reducing its degradation and improving its selectivity.

[Figure 6 near here]

The results obtained for LGA dehydration using different LGA initial concentrations with the endcapped SiliaBond®-PSA are shown in Figures 6a, 6b and 6c. The selectivity for LGO decreases with an increase in LGA initial concentration. The decrease in the LGO selectivity with the increase in LGA initial concentration is higher for endcapped SiliaBond®-PSA compared with those obtained using PS-SBA-15. Full LGA conversion was achieved starting with 14 and 36 mM LGA, while with 89 mM LGA the

View Article Online
DOI: 10.1039/C9GC01526D

maximum conversion reached was 58%. The LGA conversion starting with 89 mM LGA reaches a plateau at 70 min. After 70 min of reaction the catalyst shows no activity for LGA consumption, the average TOF after 70 min is 0.0 ks^{-1}. While PS-SBA-15 shows a TOF of 0.0 ks^{-1} after 130 min at a conversion of 82% starting with 89 mM LGA. A comparison of Figures 4a and 4b shows that the production of water is almost the same using endcapped SiliaBond®-PSA or PS-SBA-15 when the initial concentration of LGA is 14 or 36 mM. However, the production of water is 34% lower for endcapped SiliaBond®-PSA starting with 89 mM LGA. This difference suggests that the deactivation of the endcapped SiliaBond®-PSA is faster compared to PS-SBA-15 and less water is required for its complete deactivation. As mentioned above, the presence of silyl ether groups makes the endcapped SiliaBond®-PSA hydrophobic. PS-SBA-15 has a surface with a large concentration of hydroxyl groups that makes it hydrophilic. Hence, the difference in the deactivation of endcapped SiliaBond®-PSA and PS-SBA-15 starting with 89 mM LGA may be attributed to the presence of hydroxyl groups on the SBA-15 surface. The hydroxyl groups promote an interaction of water with the catalyst surface reducing its interplay with the acid sites that delay the catalyst deactivation.

Figure 7 shows the effect of the initial LGA concentration on the TOF for the consumption of LGA and the TOF for LGO production using PS-SBA-15 and endcapped SiliaBond®-PSA as catalysts. The TOFs for LGA and LGO both increase as the LGA concentration increases. Increasing the LGA concentration increases the amount of LGO and water produced during the reaction. We speculate that the difference in the TOFs for LGA and LGO at high LGA concentrations between PS-SBA-15 and endcapped SiliaBond®-PSA can be attributed to an increase in the water concentration promoting an

View Article Online
DOI: 10.1039/C9GC01526D

interaction of water with the acid sites on the endcapped SiliaBond®-PSA. The presence of silanol groups on PS-SBA-15 may promote an interaction between water and the catalyst surface, reducing the interaction of water with the acid site at high local water concentrations. On the endcapped SiliaBond®-PSA surface, the absence of the silanol groups reduces the interaction of water with the catalyst surface, but the interaction of water with the acid sites may be higher at high local water concentrations.

[Figure 7 near here]

The effect of the sulfonic group linker was also evaluated comparing the catalytic performance of two endcapped SiliaBond® functionalized catalysts, one with propylsulfonic acid (SiliaBond-PSA) and the other with arenesulfonic acid (SiliaBond®-Tosic-a) as shown in Figures 8 and 6a. The LGO selectivity at 100% LGA conversion obtained using endcapped SiliaBond®-Tosic-a was lower (52%) compared to the LGO selectivity (59%) with endcapped SiliaBond®-PSA. The selectivity for non-detectable products at 100% LGA conversion obtained with the endcapped SiliaBond®-Tosic-a was 42%, and this selectivity was 34% using endcapped SiliaBond®-PSA. The average TOF for the consumption of LGA was 3.27 ks^{-1} for the endcapped SiliaBond®-Tosic-a and equal to 2.7 ks^{-1} for the endcapped SiliaBond®-PSA. These results indicate that the activity for LGA conversion of the endcapped SiliaBond®-Tosic-a is higher compared to that for the endcapped SiliaBond®-PSA. The difference in the LGO and non-detectable products selectivities can be attributed to the difference in catalyst's activity. The endcapped SiliaBond®-Tosic-a has a higher activity and promotes the formation of non-detectable products affecting the selectivity towards LGO. The higher activity for LGA consumption observed for SiliaBond®-Tosic-a can be attributed to a higher pKa of the arenesulfonic acid

View Article Online
DOI: 10.1039/C9GC01526D

functional group compared to propylsulfonic acid. The terminal sulfonic acid group on SiliaBond®-Tosic-a is similar to benzenesulfonic acid which has a pKa of -6.5, while the terminal sulfonic acid group on SiliaBond®-PSA is similar to methanesulfonic acid which has a pKa of -2.[35] Based on those acid strengths the acid sites on SiliaBond®-Tosic-a should be stronger than those on SiliaBond®-PSA endcapped, and as a consequence more active. However, this higher acid strength may also promote the degradation of LGO.

[Figure 8 near here]

In summary, the absence of products using non-functionalized SBA-15 and the preferential production of LGO using 1-propanesulfonic acid shows that the propylsulfonic acid on the functionalized PS-SBA-15 catalyzes the conversion of LGA to LGO. Propylsulfonic functionalized silica catalysts have twice the rate of LGA conversion compared to sulfuric acid. The dehydration activity of the catalysts affects the selectivity towards LGO; catalysts with high activity promote the production of non-detectable products. An increase in the initial concentration of LGA causes a reduction in the LGO selectivity. However, the TOF for the consumption of LGA and the TOF for LGO production increase with an increment in the LGA initial concentration. This behavior is higher using PS-SBA-15 compared to the commercial endcapped SiliaBond®-PSA but both catalysts seem to deactivate at some point when the reaction starts with 89 mM LGA. The deactivation of the catalysts is related to the production of water during the reaction. The deactivation of endcapped SiliaBond®-PSA is faster and requires less water compared to PS-SBA-15. This difference suggests that the catalyst surface hydrophilicity reduces the interaction of water with the acid sites retarding the catalyst deactivation.

View Article Online
DOI: 10.1039/C9GC01526D

3.3. Thermal stability of propylsulfonic functionalized silica in THF

It has been reported that acid functionalized silica catalysts are not thermally stable in the presence of water.[29,36] It has also been demonstrated that the incorporation of hydrophobic species on silica surfaces helps to improve its stability and reduce the physicochemical changes in water environments.[34] To measure the stability of propylsulfonic acid functionalized silica catalysts in THF, the PS-SBA-15 and SiliaBond®-PSA catalysts were exposed to a series of thermal treatments in THF at 483 K and 69 bar He. Table 2 shows a summary of the physicochemical properties obtained for PS-SBA-15 and SiliaBond® catalysts after thermal treatments in THF at 483 K. A decrease in the acid sites concentration was observed when the samples were treated for 40 and 70 min. When the samples were treated for 100 min the acid concentration was almost the same to that obtained at 70 min. The acid concentration on PS-SBA-15 and SiliaBond®-PSA catalysts decreases around 15% for PS-SBA-15 and 10% for the non-endcapped and endcapped SiliaBond®-PSA catalysts. This loss can be attributed to acid site leaching during the thermal treatment in THF. The non-endcapped and the endcapped SiliaBond®-PSA catalysts have almost the same loss in acidity. This result suggests that the hydrophobic functional groups on the endcapped catalysts do not protect the acid from leaching in THF.

Table 2. Physicochemical properties of solid acid catalysts after treatment in THF at 483 K.[a]

Catalyst	Time[b] (min)	S:Si[c]	C_{H+}[d] (mmol/g)	S_{BET} (m^2/g)	S_{Ext}[e] (m^2/g)	D_p (nm)	$V_{P/Po=0.99}$ (cm^3/g)	V_p[e] (cm^3/g)	V_m[e] (cm^3/g)
PS-SBA-15	0	0.06	0.96	734	26	5.8	0.631	0.587	0.001
PS-SBA-15	40	-	0.87	1,439	48	5.8	1.261	1.170	0.013
PS-SBA-15	70	0.07	0.80 (0.82)[f]	621	24	5.8	0.551	0.511	0.004
PS-SBA-15	100	0.07	0.84	362	13	5.8	0.321	0.299	0.001
SiliaBond®-PSA endcapped	0	0.02	0.62	420	15	7.2	0.581	0.573	0.000
SiliaBond®-PSA endcapped	40	-	0.56	223	6	7.5	0.318	0.323	0.000
SiliaBond®-PSA endcapped	70	-	0.55	167	5	7.3	0.250	0.253	0.000
SiliaBond®-PSA endcapped	100	0.02	0.56	342	6	7.2	0.499	0.509	0.000
SiliaBond®-PSA non-endcapped	0	0.03	0.71	279	9	7.8	0.427	0.425	0.000
SiliaBond®-PSA non-endcapped	70	0.03	0.64	338	5	5.8	0.535	0.535	0.000

[a]C_{H+} is the content of Brønsted acid sites on the catalyst surface per gram of catalyst, S_{BET} is the BET surface area, S_{Ext} is the external surface area, D_p is the mesopore diameter, $V_{P/Po=0.99}$ is the total pore volume estimated from the amount of N_2 adsorbed at a relative pressure of 0.99, V_p is the mesopore volume, and V_m is the micropore volume.
[b]Time for which the catalyst was exposed to 483 K in THF at 69 bar He.
[c]Sulfur to silicon molar ratio obtained from the elemental composition determined by ICP.
[d]Determined by titration.
[e]Calculated using α_s-plot method using the standard parameters corresponding to mesoporous silica.
[f]The second value corresponds to the acidity determined for a sample treated removing 25 mL of the liquid phase during the experiment.

View Article Online
DOI: 10.1039/C9GC01526D

Figures 9 and 10 show the XRD patterns and the physisorption isotherms obtained for propylsulfonic acid functionalized silica catalysts after treatment in THF at 483 K. The physicochemical properties of the catalysts change with its exposure to THF at 483 K. For PS-SBA-15, the BET and external surface area and porosity increase after 40 min of treatment in THF, as shown in Table 2. Afterwards, the BET and external surface area and porosity decrease with an increase in the treatment time. However, the average pore diameter remains constant during all treatments. The ratio of sulfur to silicon atoms increases after 70 min treatment and remains constant at 100 min treatment. These results suggest that the increase in surface area and porosity are related to a loss in silica during the thermal treatment in THF at 483 K. These physicochemical changes do not cause significant changes to the mesostructure order, as shown in Figures 9a and 10a. The XRD pattern and the type of hysteresis obtained for the treated catalyst remains almost the same to those obtained for the untreated PS-SBA-15.

[Figure 9 near here]

[Figure 10 near here]

The surface areas, average mesopore diameter and volume vary with the treatment time for the endcapped and non-endcapped SiliaBond®-PSA catalysts. However, the ratio of sulfur to silicon remains constant in contrast to PS-SBA-15. Apparently, the silicon of the SiliaBond® catalysts is not dissolving in the THF. The XRD pattern and the type of hysteresis obtained for the treated SiliaBond®-PSA catalysts remains almost the same to those obtained for the untreated SiliaBond®-PSA. These results suggest that these physicochemical changes do not cause significant changes to the partial order of the pores, as observed in PS-SBA-15.

View Article Online
DOI: 10.1039/C9GC01526D

PS-SBA-15 was also treated in THF for 70 min at 483 K partially removing the solvent during the treatment. The acid concentration of this catalyst was measured after each treatment. This experiment was performed to corroborate that the functional groups remain on the catalyst surface during the reaction and were not removed at the reaction temperature and readsorbed on the catalyst surface during the ice bath quench. The total THF removed during the treatment was 25.5 mL. The acid concentration after this treatment was 0.82 mmol H^+/g, almost the same obtained for the catalyst treated without removing the THF during treatment (0.80 mmol H^+/g). This result confirms that the functional groups remain on the catalyst surface during reaction and the functional group is not present in the solvent and acting as a homogeneous catalyst.

4. Conclusions

The dehydration of LGA to LGO was studied using Brønsted solid acid catalysts in tetrahydrofuran (THF). LGO selectivities of up to 68% are obtained using propylsulfonic acid functionalized catalysts. The production of water during the reaction affects the catalytic behavior of the acid group due to a stabilization of the acid proton. Using a solid acid catalyst with hydroxyl groups on the surface such as PS-SBA-15 reduces this effect, allowing the achievement of higher LGA conversion and LGO selectivity. The structural properties and surface hydrophobicity and hydrophilicity do not have an effect on the acid site activity. The acidity of the PS-SBA-15 and SiliaBond® catalysts in THF at the reaction temperature appears to be stable. The PS-SBA-15 physicochemical changes can be mainly attributed to the loss of Si during the temperature treatment in THF. This study shows that the use of Brønsted solid acid catalysts improves the production of LGO from LGA and

View Article Online
DOI: 10.1039/C9GC01526D

provides insights regarding the catalytic properties needed for the selective production of LGO from LGA.

Conflicts of interest

There are no conflicts to declare.

Acknowledgements

This work was supported through the NSF CREST: Nanotechnology Center for Biomedical, Environment and Sustainability Applications - Phase II (Award HRD-1345156) and the DOE EERE: Office of Energy Efficiency and Renewable Energy (Award DE-EE0006878). We wish to also acknowledge partial support from the NSF funded RII Track-2 FEC: Center for a Sustainable Water, Energy, and Food Nexus (Award OIA-1632824).

References

1 D. M. Alonso, J. Q. Bond and J. A. Dumesic, *Green Chem.*, 2010, **12**, 1493.

2 C.-H. Zhou, X. Xia, C.-X. Lin, D.-S. Tong and J. Beltramini, *Chem. Soc. Rev.*, 2011, **40**, 5588.

3 S. G. Wettstein, D. M. Alonso, E. I. Gürbüz and J. A. Dumesic, *Curr. Opin. Chem. Eng.*, 2012, **1**, 218–224.

4 M. J. Climent, A. Corma and S. Iborra, *Green Chem.*, 2014, **16**, 516.

5 F. Cao, T. J. Schwartz, D. J. McClelland, S. H. Krishna, J. A. Dumesic and G. W. Huber, *Energy Env. Sci*, 2015, **8**, 1808–1815.

6 Biomass Explained, http://www.eia.gov/energyexplained/?page=biomass_home.

7 O. Oyola-Rivera, A. M. González-Rosario and N. Cardona-Martínez, *Biomass Bioenergy*, 2018, **119**, 284–292.

8 J. He, M. Liu, K. Huang, T. W. Walker, C. T. Maravelias, J. A. Dumesic and G. W. Huber, *Green Chem*, 2017, **19**, 3642–3653.

9 A. M. Sarotti, R. A. Spanevello and A. G. Suárez, *Green Chem.*, 2007, **9**, 1137.

View Article Online
DOI: 10.1039/C9GC01526D

10 Z. Wang, Q. Lu, X.-F. Zhu and Y. Zhang, *ChemSusChem*, 2011, **4**, 79–84.

11 S. Kudo, Z. Zhou, K. Norinaga and J. Hayashi, *Green Chem.*, 2011, **13**, 3306.

12 M. Ostermeier and R. Schobert, *J. Org. Chem.*, 2014, **79**, 4038–4042.

13 C. Müller, M. A. Gomez-Zurita Frau, D. Ballinari, S. Colombo, A. Bitto, E. Martegani, C. Airoldi, A. S. van Neuren, M. Stein, J. Weiser, C. Battistini and F. Peri, *ChemMedChem*, 2009, **4**, 524–528.

14 M. De bruyn, J. Fan, V. L. Budarin, D. J. Macquarrie, L. D. Gomez, R. Simister, T. J. Farmer, W. D. Raverty, S. J. McQueen-Mason and J. H. Clark, *Energy Environ. Sci.*, 2016, **9**, 2571–2574.

15 A. Broido, M. Evett and C. C. Hodges, *Carbohydr. Res.*, 1975, **44**, 267–274.

16 Y. Halpern, R. Riffer and A. Broido, *J. Org. Chem.*, 1973, **38**, 204–209.

17 F. Shafizadeh, R. H. Furneaux and T. T. Stevenson, *Carbohydr. Res.*, 1979, **71**, 169–191.

18 C. M. Lakshmanan and H. E. Hoelscher, *Ind. Eng. Chem. Prod. Res. Dev.*, 1970, **9**, 57–59.

19 H. Kawamoto, S. Saito and S. Saka, *J. Anal. Appl. Pyrolysis*, 2008, **82**, 78–82.

20 J. Zandersons, A. Zhurinsh, G. Dobele, V. Jurkjane, J. Rizhikovs, B. Spince and A. Pazhe, *J. Anal. Appl. Pyrolysis*, 2013, **103**, 222–226.

21 D. Carpenter, T. L. Westover, S. Czernik and W. Jablonski, *Green Chem*, 2014, **16**, 384–406.

22 M. A. Mellmer, C. Sener, J. M. R. Gallo, J. S. Luterbacher, D. M. Alonso and J. A. Dumesic, *Angew. Chem. Int. Ed.*, 2014, **53**, 11872–11875.

23 D. Margolese, J. A. Malero, S. C. Christiansen, B. F. Chmelka and G. D. Stucky, *Chem. Mater.*, 2000, **12**, 2448–2459.

24 V. Pandarus, G. Gingras, F. Béland, R. Ciriminna and M. Pagliaro, *Catal. Sci. Technol.*, 2011, **1**, 1600.

25 A. Sayari, P. Liu, M. Kruk and M. Jaroniec, *Chem. Mater.*, 1997, **9**, 2499–2506.

26 M. Kruk, M. Jaroniec and A. Sayari, *Chem. Mater.*, 1999, **11**, 492–500.

27 M. Kruk, M. Jaroniec, C. H. Ko and R. Ryoo, *Chem. Mater.*, 2000, **12**, 1961–1968.

View Article Online
DOI: 10.1039/C9GC01526D

28 M. Jaroniec and L. A. Solovyov, *Langmuir*, 2006, **22**, 6757–6760.

29 D. Reyes-Luyanda, J. Flores-Cruz, P. J. Morales-Pérez, L. G. Encarnación-Gómez, F. Shi, P. M. Voyles and N. Cardona-Martínez, *Top. Catal.*, 2012, **55**, 148–161.

30 S. Ravi, R. Roshan, J. Tharun, A. C. Kathalikkattil and D. W. Park, *J. CO2 Util.*, 2015, **10**, 88–94.

31 S. Hamoudi and S. Kaliaguine, *Microporous Mesoporous Mater.*, 2003, **59**, 195–204.

32 R. B. Babou Kammoe and S. Hamoudi, *J. Environ. Qual.*, 2014, **43**, 1032.

33 K. Leung, I. M. B. Nielsen and L. J. Criscenti, *J. Am. Chem. Soc.*, 2009, **131**, 18358–18365.

34 G. Morales, G. Athens, B. Chmelka, R. Vangrieken and J. Melero, *J. Catal.*, 2008, **254**, 205–217.

35 E. P. Serjeant, B. Dempsey and International Union of Pure and Applied Chemistry, Eds., *Ionization constants of organic acids in aqueous solutions*, Pergamon Press, Oxford ; New York, 1979.

36 M. H. Tucker, A. J. Crisci, B. N. Wigington, N. Phadke, R. Alamillo, J. Zhang, S. L. Scott and J. A. Dumesic, *ACS Catal.*, 2012, **2**, 1865–1876.

View Article Online
DOI: 10.1039/C9GC01526D

List of Figures

View Article Online
DOI: 10.1039/C9GC01526D

Figure 7. Effect of LGA concentration on average TOF (a) of LGA consumption and (b) of LGO production using PS-SBA-15 and SiliaBond®-PSA catalysts in THF at 483 K and 69 bar. The acid loading was kept at 0.08 mmol H^+.

Figure 8. Dehydration of 14 mM LGA using endcapped SiliaBond®-Tosic-a catalyst in THF at 483 K and 69 bar He with an acid loading of 0.08 mmol H^+.

Figure 9. Powder XRD pattern for functionalized silica with propyl sulfonic acid after thermal treatment in THF at 483 K: (a) PS-SBA-15 and (b) SiliaBond®-PSA endcapped.

Figure 10. N_2 adsorption and desorption isotherms for functionalized silica with propyl sulfonic acid after thermal treatment in THF at 483 K. Results for (a) PS-SBA-15 and (b) SiliaBond®-PSA endcapped.

View Article Online
DOI: 10.1039/C9GC01526D

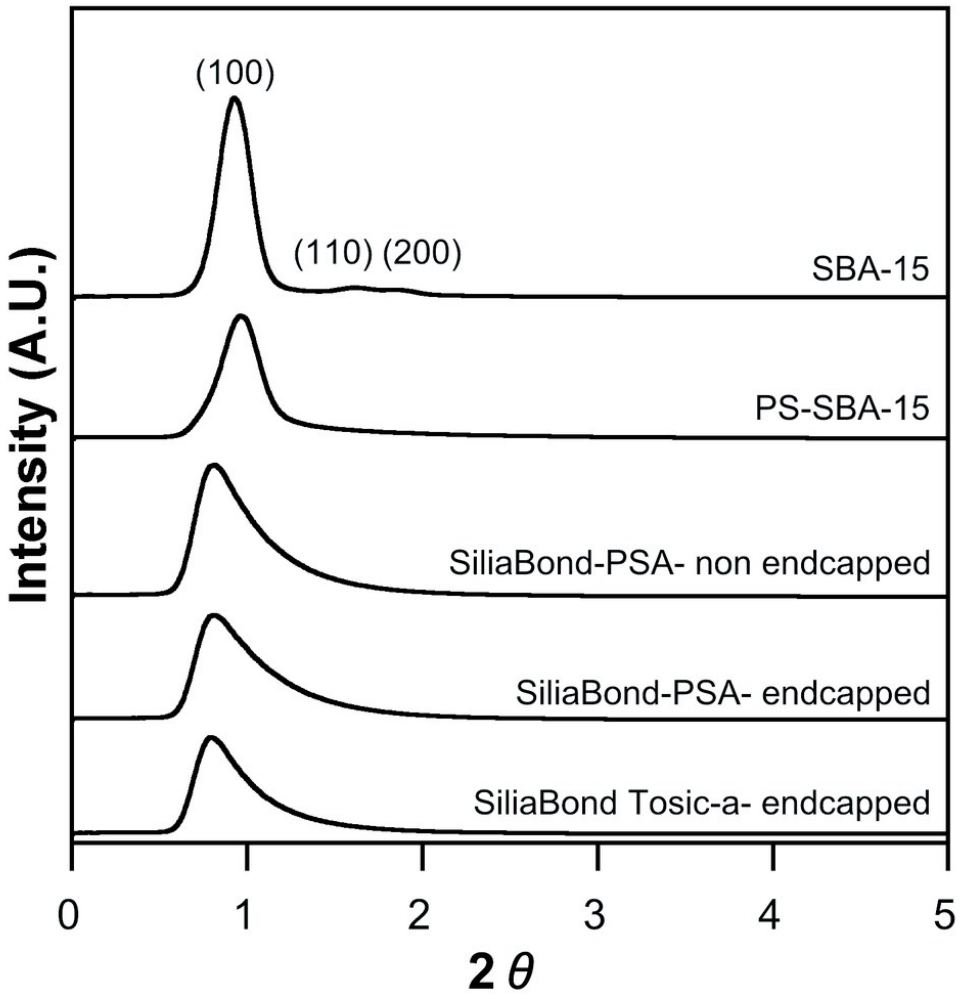

Figure 1. Powder XRD patterns for silica catalysts functionalized with sulfonic acid groups.

82x82mm (300 x 300 DPI)

View Article Online
DOI: 10.1039/C9GC01526D

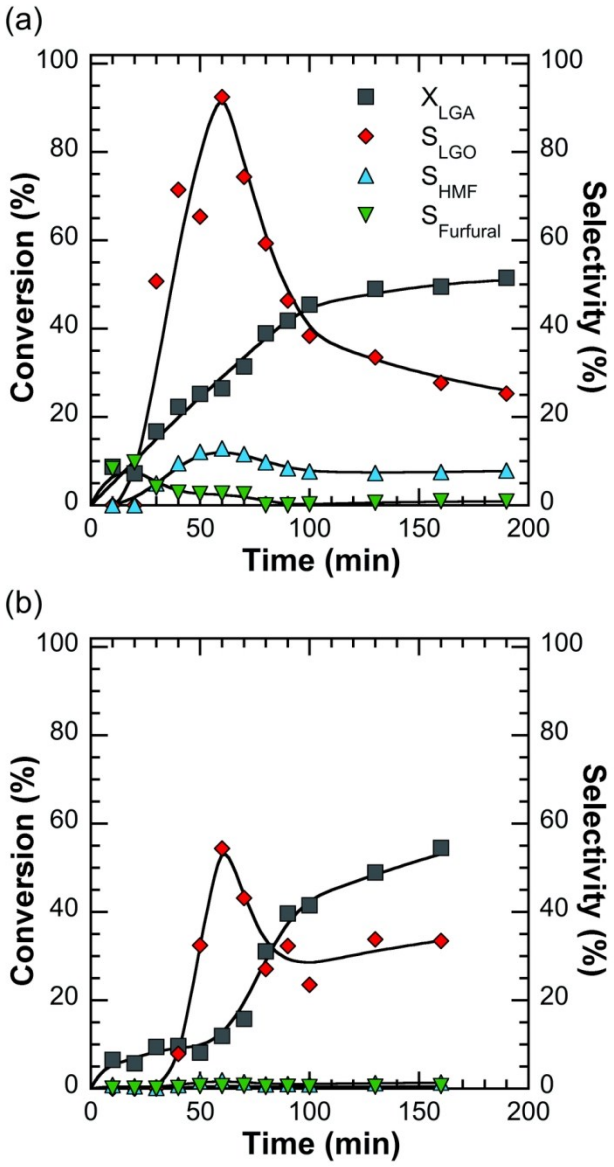

Figure 2. Dehydration of 14 mM LGA using homogeneous acid catalysts: (a) H_2SO_4 and (b) 1-propanesulfonic acid in THF at 483 K and 69 bar He with 0.08 mmol H^+.

82x161mm (300 x 300 DPI)

View Article Online
DOI: 10.1039/C9GC01526D

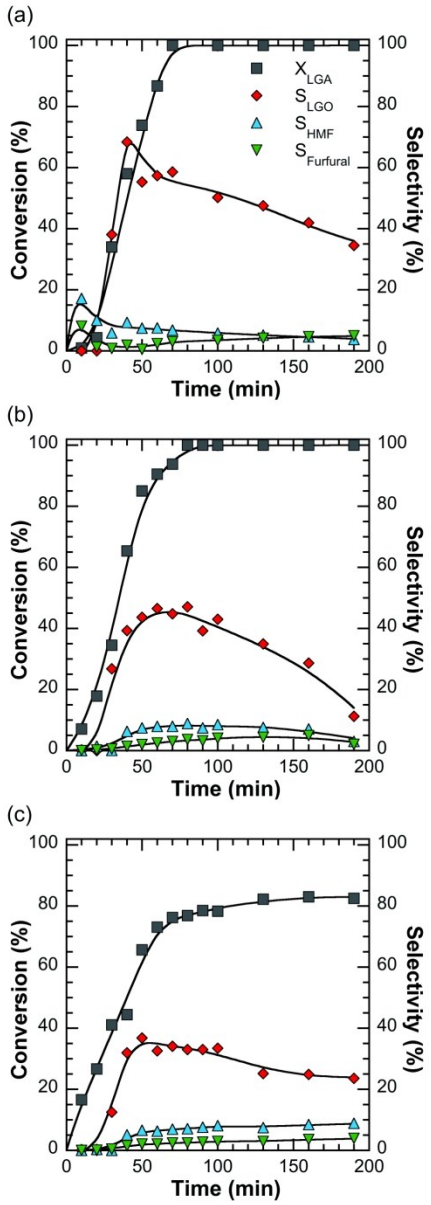

Figure 3. Effect of LGA concentration on the dehydration of LGA using PS-SBA-15 catalyst in THF at 483 K and 69 bar He and LGA concentrations of (a) 14 mM, (b) 36 mM, and (c) 89 mM. The acid loading was kept to 0.08 mmol H^+.

82x233mm (300 x 300 DPI)

View Article Online
DOI: 10.1039/C9GC01526D

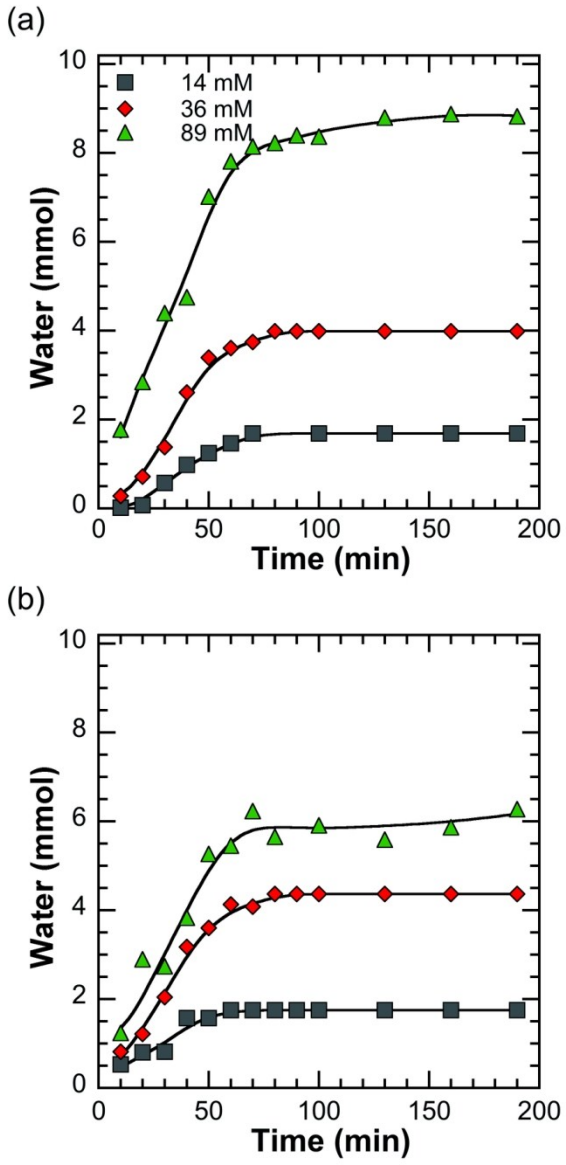

Figure 4. Water production during the dehydration of LGA for different LGA initial concentrations in THF at 483 K and 69 bar He and catalysts: (a) PS-SBA-15 and (b) SiliaBond-PSA endcapped.

82x160mm (300 x 300 DPI)

View Article Online
DOI: 10.1039/C9GC01526D

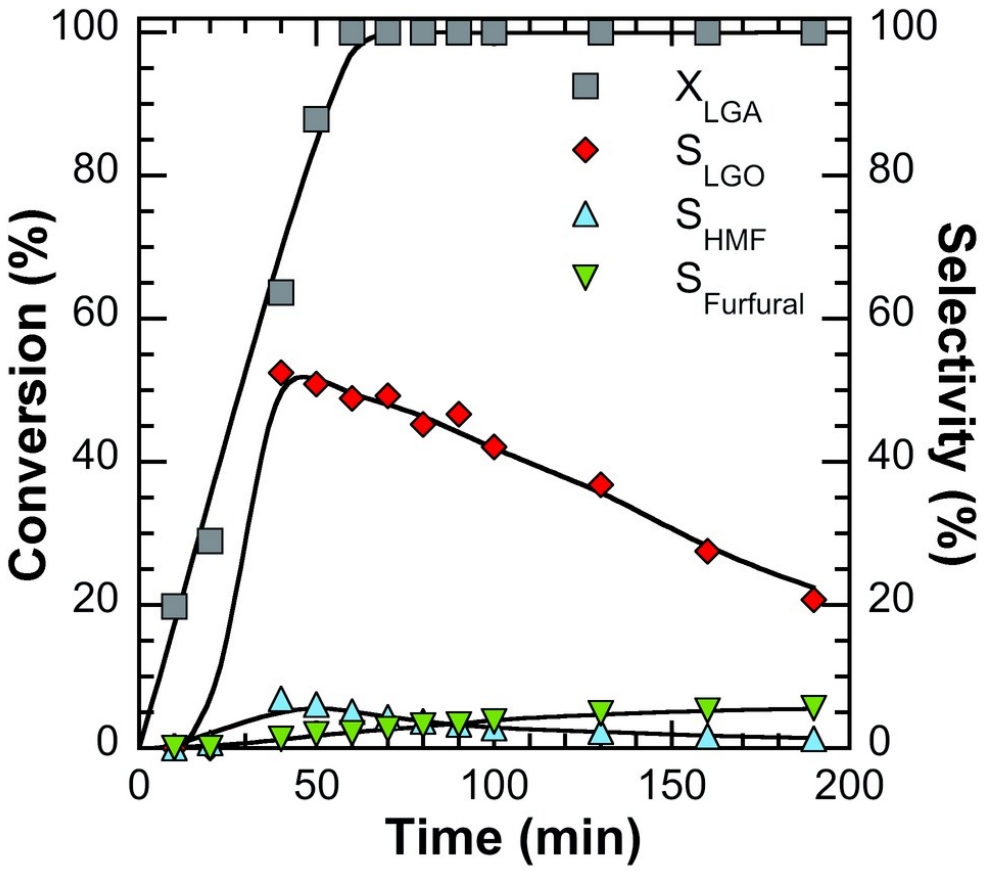

Figure 5. Dehydration of 14 mM LGA using non-endcapped SiliaBond®-PSA catalyst in THF at 483 K and 69 bar He with an acid loading of 0.08 mmol H^+.

82x82mm (300 x 300 DPI)

View Article Online
DOI: 10.1039/C9GC01526D

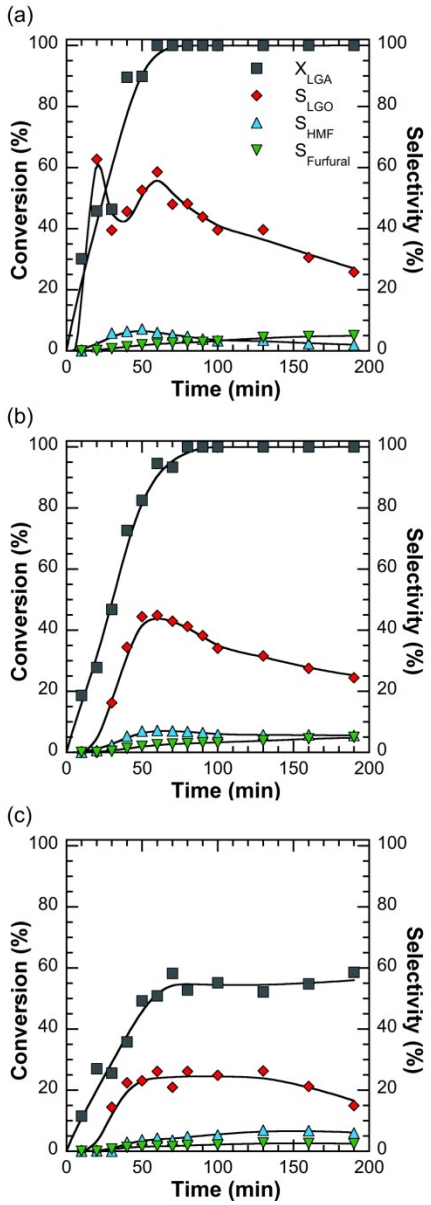

Figure 6. Effect of LGA concentration on the dehydration of LGA using endcapped SiliaBond®-PSA catalyst in THF at 483 K and 69 bar He. The acid loading was kept at 0.08 mmol H^+. The LGA concentrations were: (a) 14 mM, (b) 36 mM and (c) 89 mM.

82x233mm (300 x 300 DPI)

View Article Online
DOI: 10.1039/C9GC01526D

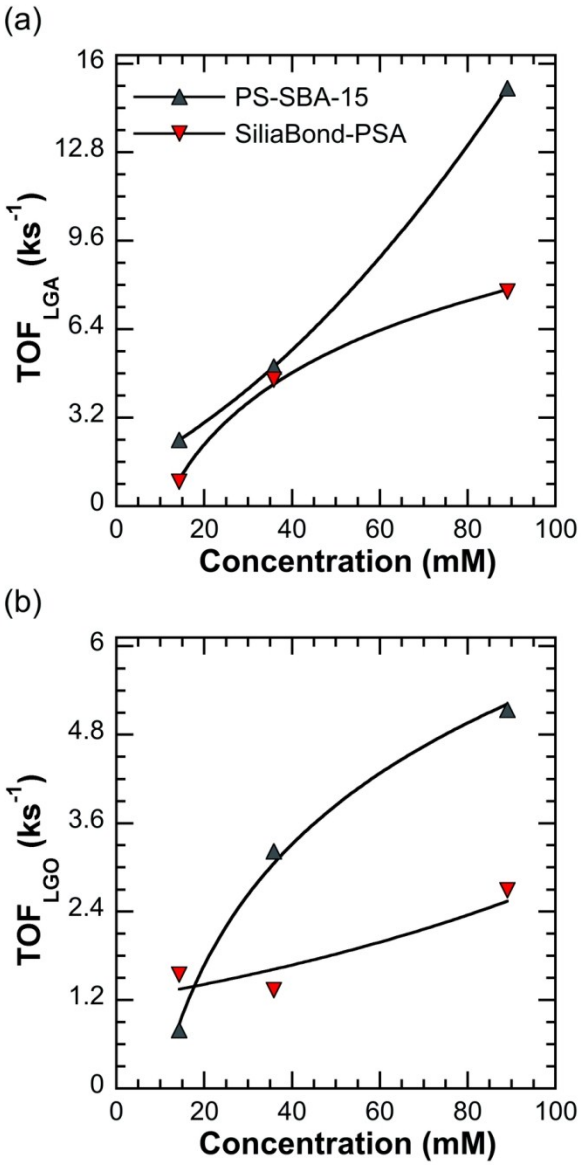

Figure 7. Effect of LGA concentration on average TOF (a) of LGA consumption and (b) of LGO production using PS-SBA-15 and SiliaBond®-PSA catalysts in THF at 483 K and 69 bar. The acid loading was kept at 0.08 mmol H^+.

82x160mm (300 x 300 DPI)

View Article Online
DOI: 10.1039/C9GC01526D

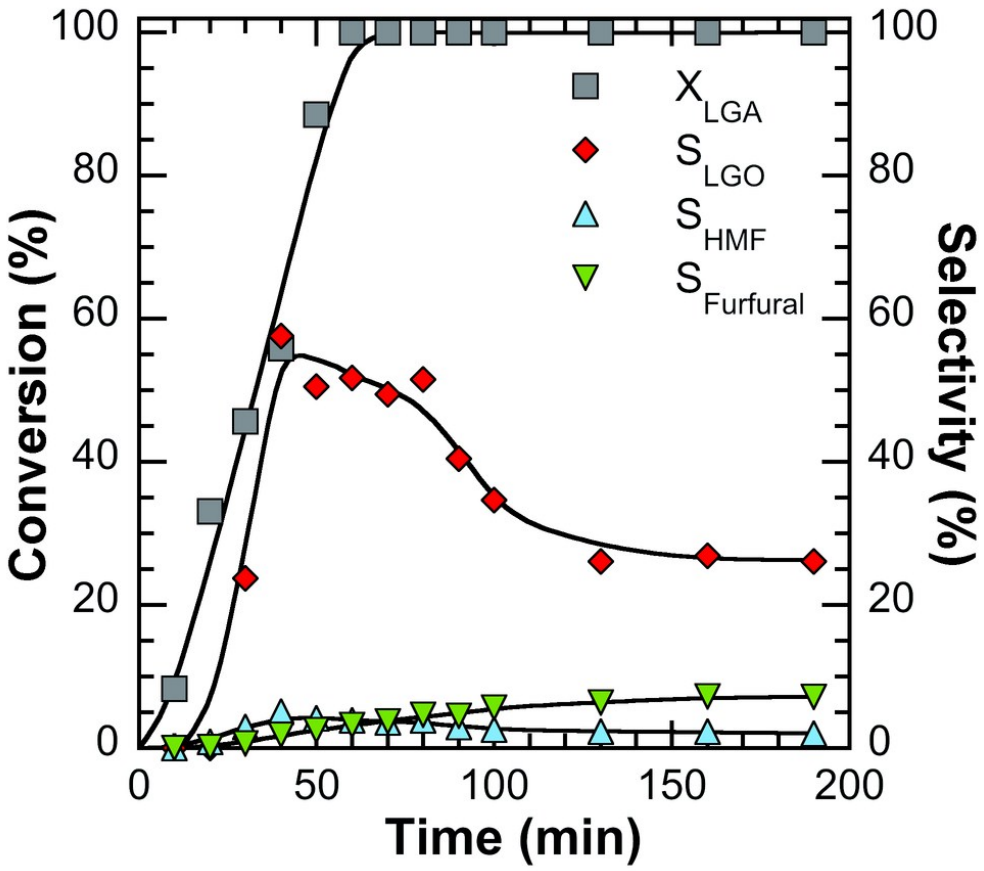

Figure 8. Dehydration of 14 mM LGA using endcapped SiliaBond®-Tosic-a catalyst in THF at 483 K and 69 bar He with an acid loading of 0.08 mmol H^+.

82x82mm (300 x 300 DPI)

View Article Online
DOI: 10.1039/C9GC01526D

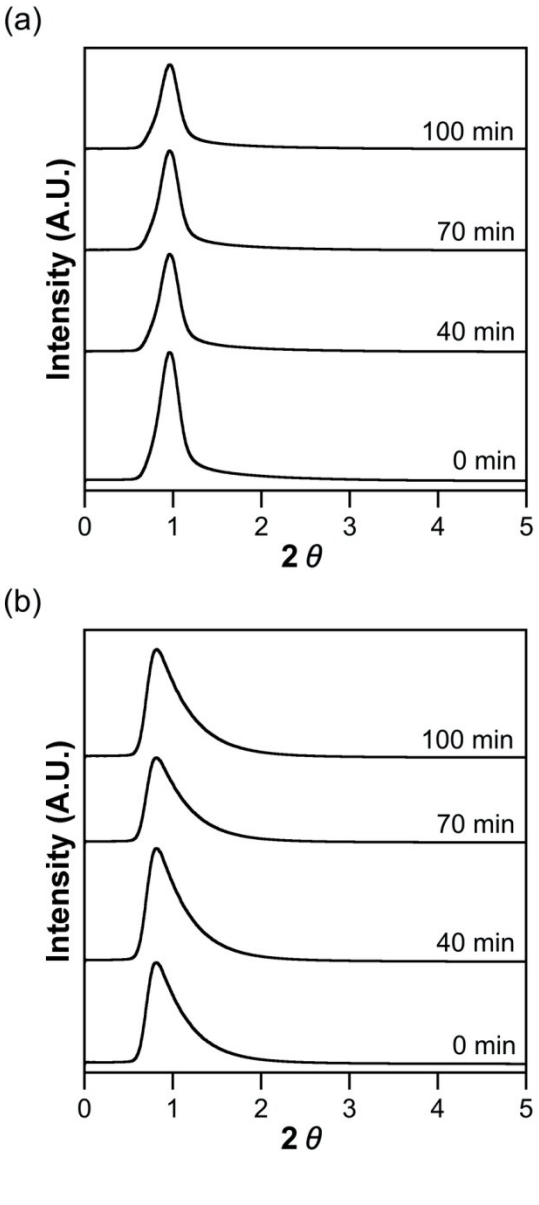

Figure 9. Powder XRD pattern for functionalized silica with propyl sulfonic acid after thermal treatment in THF at 483 K: (a) PS-SBA-15 and (b) SiliaBond®-PSA endcapped.

82x160mm (300 x 300 DPI)

View Article Online
DOI: 10.1039/C9GC01526D

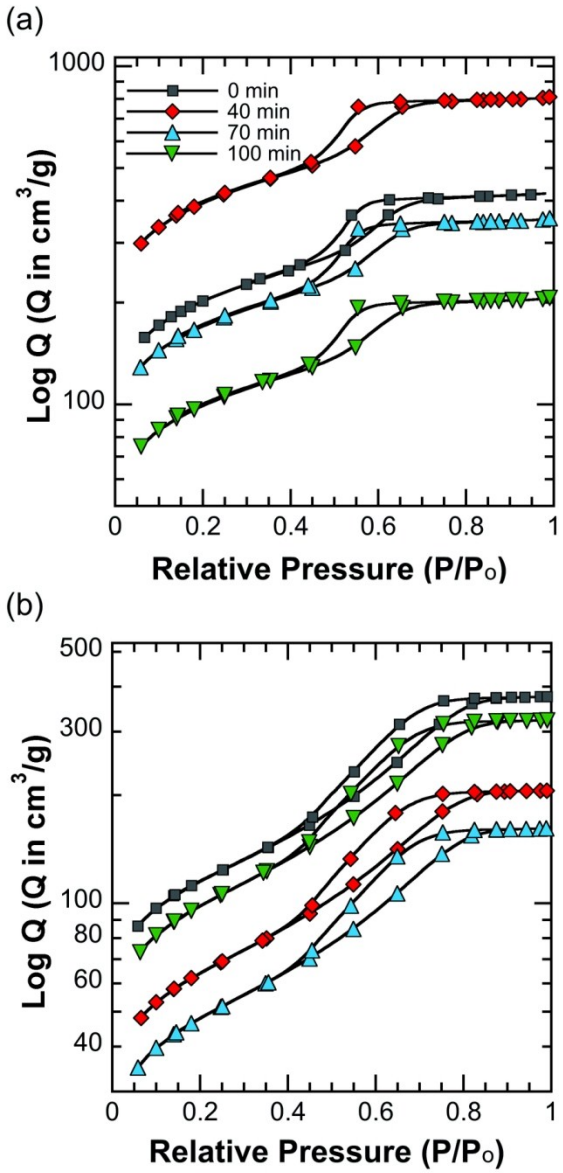

Figure 10. N_2 adsorption and desorption isotherms for functionalized silica with propyl sulfonic acid after thermal treatment in THF at 483 K. Results for (a) PS-SBA-15 and (b) SiliaBond®-PSA endcapped.

82x161mm (300 x 300 DPI)

View Article Online
DOI: 10.1039/C9GC01526D

Graphical Abstract

We explored the production of levoglucosenone from levoglucosan using propylsulfonic acid functionalized silica; 59% selectivity was obtained at 100% conversion.